Mallia, A. K., John, J., Lakshmanan, M. R., Jungalwala, F. B., & Cama, H. R. (1970) *Indian J. Biochem. 7*, 102–103.
McCormick, A. M., & Napoli, J. L. (1982) *J. Biol. Chem. 257*, 1730–1735.
McCormick, A. M., Napoli, J. L., Schnoes, H. K., & De Luca, H. F. (1978) *Biochemistry 17*, 4805–4090.
McCormick, A. M., Napoli, J. L., Yoshizawa, S., & De Luca, H. F. (1980) *Biochem. J. 186*, 475–481.
Morgan, B., & Thompson, J. N. (1966) *Biochem. J. 101*, 835–842.
Napoli, J. L., & McCormick, A. M. (1981) *Biochim. Biophys. Acta 666*, 165–175.
Napoli, J. L., McCormick, A. M., Schnoes, H. K., & De Luca, H. F. (1978) *Proc. Natl. Acad. Sci. U.S.A. 75*, 2603–2605.
Newton, D. L., Henderson, W. R., & Sporn, M. B. (1980) *Cancer Res. 40*, 3413–3425.
Rietz, P., Wiss, O., & Weber, F. (1974) *Vitam. Horm. (N.Y.) 32*, 237–249.
Roberts, A. B., Nichols, M. D., Frolik, C. A., Newton, D. L., & Sporn, M. B. (1978) *Cancer Res. 38*, 3327–3332.
Roberts, A. B., Frolik, C. A., Nichols, M. D., & Sporn, M. B. (1979) *J. Biol. Chem. 254*, 6303–6309.
Sporn, M. B., Dunlop, N. M., Newton, D. L., & Henderson, W. R. (1976) *Nature (London) 263*, 110–113.
Strickland, S. (1978) *Cold Spring Harbor Conf. Cell Proliferation 6*, 671–676.
Strickland, S., & Mahdavi, V. (1980) *Cell (Cambridge, Mass.) 15*, 393–403.
Verma, A. K., Slaga, T. J., Wertz, P. W., Mueller, G. C., & Boutwell, R. K. (1980) *Cancer Res. 40*, 2367–2371.
Zile, M., Schnoes, H. K., & De Luca, H. F. (1980) *Proc. Natl. Acad. Sci. U.S.A. 77*, 3230–3233.

Kinetic and Mechanistic Analysis of Prothrombin–Membrane Binding by Stopped-Flow Light Scattering†

G. Jason Wei, Victor A. Bloomfield, Robert M. Resnick, and Gary L. Nelsestuen*

ABSTRACT: We have investigated the kinetics and mechanism of prothrombin–membrane vesicle interaction by using stopped-flow light scattering. Under conditions of approximately physiological protein concentration (≤3 μM prothrombin), prothrombin interaction with the vesicles was modeled according to a simple bimolecular process with noninteracting prothrombin binding sites on the vesicle. The association rate constant (per protein binding site) for interaction of prothrombin with vesicles containing 20% phosphatidylserine–80% phosphatidylcholine at 10 °C, in buffer containing 3 mM calcium, is $(1 \pm 0.1) \times 10^7$ $M^{-1} \cdot s^{-1}$. This corresponds to a 10% collision efficiency. The reverse process is a first-order dissociation with a rate constant of 3 ± 1 s^{-1}. Off-rate experiments conducted by sample dilution were consistent with these values. With varying membrane compositions the association process was found to be somewhat cooperative with respect to phosphatidylserine, but dissociation was unaffected by phosphatidylserine density. The activation energy for prothrombin–membrane association varied with the amount of acidic phospholipid in the membrane. Membranes of 10% phosphatidylserine gave an activation energy of about 9 kcal/mol while those of 40% phosphatidylserine gave a value of 4 kcal/mol. For these same membranes the collision efficiency was estimated to be 3 and 20%, respectively. This trend in the activation energy suggests that as the acidic phospholipid content increases, the association energy of activation becomes characteristic of a diffusion-controlled reaction. Dissociation rate constants were obtained by mixing prothrombin–membrane complexes with ethylene glycol bis-(β-aminoethyl ether)-*N,N,N′,N′*-tetraacetic acid (EGTA). It was found that a necessary population of calcium ions exchanged rapidly from the prothrombin–membrane complex but that this population could be replaced by magnesium or manganese. A second population of essential ions, specific for calcium, exchanged slowly and, under certain conditions, appeared to be released at the rate of prothrombin–membrane dissociation. Under conditions of high free-protein concentrations the association process became complex and had lower rate constants. The anomalous binding characteristics were observed under conditions that are not likely to be physiologically important.

The blood coagulation cascade contains several enzymatic steps that are dependent on the presence of a phospholipid membrane component [see Jackson & Nemerson (1980) for a review]. Both the substrates and enzymes in these reactions are vitamin K dependent proteins that show calcium-dependent binding to the phospholipid membrane in a process that depends on γ-carboxyglutamic acid residues. Understanding of the kinetic processes involved in blood coagulation therefore requires knowledge of these protein–membrane interactions.

Previous studies have revealed much about the interaction of vitamin K dependent proteins with membranes at equilibrium. For the protein prothrombin, binding constants under a variety of conditions have been reported (Nelsestuen & Lim, 1977; Nelsestuen & Broderius, 1977; Nelsestuen et al., 1978; Resnick & Nelsestuen, 1980). Independent studies have dealt with the binding of prothrombin fragment 1 (residues 1–156 of prothrombin) to phospholipid vesicles (Dombrose et al., 1979). These proteins appear to bind to the surface of the phospholipid without penetration into the hydrophobic region of the membrane (Lim et al., 1977; Hanahan et al., 1969). Dissociation constants for binding to membranes containing approximately physiological amounts of acidic phospholipid, which are similar to cytosolic membranes, at physiological calcium concentration, are very near to the plasma concen-

† From the Department of Biochemistry, College of Biological Sciences, University of Minnesota, St. Paul, Minnesota 55108. *Received June 11, 1981.* This work was supported in part by Grant HL 15728 from the National Institutes of Health (to G.L.N.) and Grant PCM 78-06777 from the National Science Foundation (to V.A.B.).

0006-2960/82/0421-1949$01.25/0 © 1982 American Chemical Society

trations of prothrombin (Nelsestuen & Broderius, 1977). These binding constants have been compared to the kinetics of thrombin formation in an attempt to establish the mechanism of enzyme–substrate interaction in this complex process [e.g., Nelsestuen (1978), Nesheim et al. (1979), and Rosing et al. (1980)].

For full understanding, knowledge of the dynamic aspects of protein–membrane interaction is equally important. This paper reports the use of stopped-flow light scattering intensity changes to measure rapid protein–membrane interactions. We have modeled the data according to a simple bimolecular interaction between protein and phospholipid. Kinetics of binding under a variety of conditions provide insight into the properties of this protein–membrane interaction.

Materials and Methods

Prothrombin was prepared and quantitated as described previously (Nelsestuen & Lim, 1977). Single bilayer phospholipid vesicles were prepared by a slight modification (Nelsestuen & Lim, 1977) of the method of Huang (1969). The phospholipids were purchased from the Sigma Chemical Co. and are reported to be greater than 95% pure. Phospholipid purity was ascertained by HPLC[1] chromatography on a 0.4 × 30 cm CN-10 (Varian Instruments, Inc.) column with phospholipid detection by its absorbance at 207 nm. This is similar to the method of Hax & Geurts van Kessel (1977). Purity was confirmed by thin-layer chromatography and analysis for phosphate compounds (Bunn et al., 1969). Phospholipid vesicle size was determined with QLS analysis as described elsewhere (Bloomfield & Lim, 1978). Unless indicated otherwise, the buffer system used was 0.05 M Tris (pH 7.5)–0.1 M NaCl.

Equilibrium Measurements. Measurements of protein–phospholipid binding at equilibrium were accomplished by relative light scattering intensity measurements at 90°. Where instrumental and solution conditions are identical and light scattering from the buffer solution is subtracted, the ratio of light scattering intensities of two solutions containing particles much smaller than the wavelength of light becomes

$$\frac{I_{s_2}}{I_{s_1}} = \frac{(\partial n/\partial c)_2^2 M_{r_2} c_2 (1 + 2B_1 c_1)}{(\partial n/\partial c)_1^2 M_{r_1} c_1 (1 + 2B_2 c_2)} \quad (1)$$

I_{s_i} is the light scattering intensity, $(\partial n/\partial c)_i$ is the refractive index increment, M_{r_i} is the molecular weight, B_i is the second virial coefficient, and c_i is the concentration of each light scattering species. Under the dilute solution conditions used, the second virial coefficient has previously been shown to be negligible (Nelsestuen & Lim, 1977). The method of estimating the weight average refractive index increment term in this expression has been discussed in detail previously (Nelsestuen & Lim, 1977) and contains potential errors, but, since this term contributes only a small amount to the total intensity change, the error effect is not large. This term is not a source of error for conclusions involving data comparisons.

Equation 1 was used, by methods described fully elsewhere (Nelsestuen & Lim, 1977), to measure prothrombin–membrane binding at equilibrium. This light scattering technique can be used to estimate the amounts of free and membrane-bound protein and to obtain equilibrium binding constants.

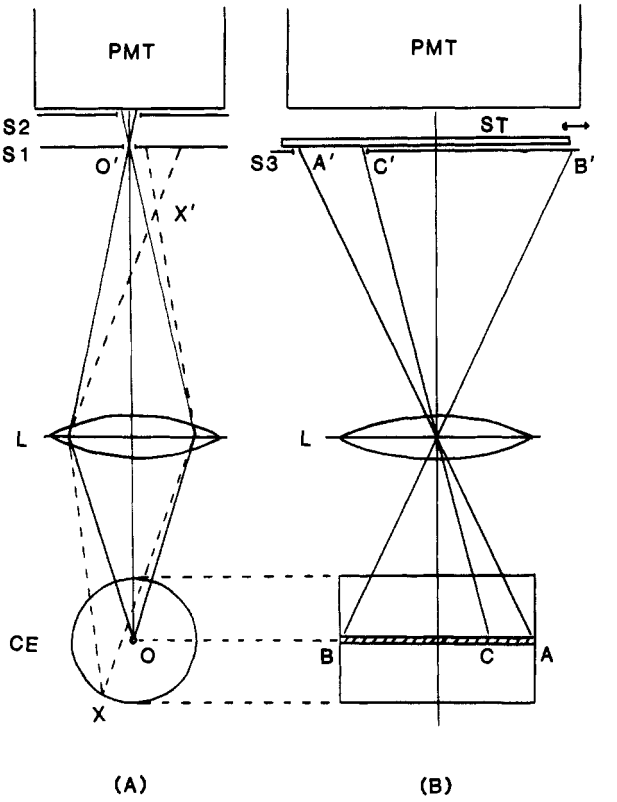

FIGURE 1: Explanation of how a slit–lens combination eliminates background scattering (A) and optimizes between scattering signal and dead time (B). Part B shows a 90° rotation of part A. PMT, photomultiplier tube; S1 and S2, slits parallel to the cell length; S3, slit perpendicular to the cell length; L, imaging lens; CE, observation cell in the stopped-flow apparatus; O, center of cell and laser beam; ACB, path of the laser beam through the cell (A end is connected to a mixing jet and B end to a stop syringe); O', A', C', and B', the images of O, A, C, B, respectively; ST, sliding shutter.

The average molecular weights of the single bilayer vesicle preparations used in this study were determined by total intensity light scattering as described in detail elsewhere (Pletcher et al., 1980). The dimensions of the phospholipid vesicles used were much smaller than the wavelength of light and should exhibit Rayleigh light scattering. To affirm this fact, we examined the angular dependence of molecular weight, and the 90° values were within 5% of the values extrapolated to zero angle. This small factor was ignored in data analysis. The diffusion constants ($D_{20,w}$) for vesicle preparations were determined by quasi-elastic light scattering (Lim et al., 1977) and were used to calculate vesicle dimensions, assuming spherical shape. The values reported are Z-averaged diffusion constants and particle radii. The $\partial n/\partial c$ for phospholipid vesicles was 0.14 cm^3/g (Yi & MacDonald, 1973).

Stopped-Flow Apparatus. The stopped-flow experiments were carried out in a Durrum D-130 mixing apparatus, equipped with a custom-designed optical and detection system. Samples were degassed under aspirator vacuum in a sonication bath for 5 min before loading into the syringes. Light from a Spectra Physics 125 He–Ne laser was focused by a lens (f = 15 cm) to produce a narrow beam through the cell. The use of a focused beam discriminates against particulate contamination and microbubbles (Liddle et al., 1977). The scattered light at 90° to the incident beam was imaged by a second lens (f = 4 cm) onto a series of three slits in front of a RCA 7265 photomultiplier tube (Figure 1). The photocurrent was amplified by a PAR 114 amplifier and digitized in a Fabri-Tek 1010 transient recorder. The recorded signal

[1] Abbreviations: PS, phosphatidylserine; PC, phosphatidylcholine; PG, phosphatidylglycerol; PE, phosphatidylethanolamine; HPLC, high-pressure liquid chromatography; Tris, tris(hydroxymethyl)aminomethane; QLS, quasi-elastic light scattering; EDTA, ethylenediaminetetraacetic acid; EGTA, ethylene glycol bis(β-aminoethyl ether)-N,N,N',N'-tetraacetic acid.

was displayed on an oscilloscope and plotted on a chart recorder for analysis. The dead time was found to be about 8 ms by mixing a solution of casein micelles and EDTA, which caused a conversion from a turbid to a clear solution with a single exponential curve. However, the data analysis used was insensitive to dead time between at least 5 and 10 ms.

As shown in Figure 1A, the combination of an imaging lens (L) and a slit (S1) eliminates most of the background scattering from the cell (CE). For example, when the center of the laser beam (O) is focused at the slit opening (O′), most of the light scattered from any point (X) on the cell wall will not reach the detector (PMT). A second slit (S2) is added to block off stray light from any other sources.

Another major advantage of using a slit–lens system is that the optimization between the scattering signal and the dead time can be achieved easily. One way to increase the magnitude of the signal is to increase the path length of the light beam. However the dead time of the instrument will also increase accordingly. By adjusting the width of slit 3 (Figure 1B), one can effectively choose a path length (starting from the mixing end) that optimizes both factors under consideration, without the trouble of replacing the cell block of the stopped-flow instrument.

Analysis of Rate Data. The rate expression for a simple bimolecular interaction of prothrombin (P) with a phospholipid vesicle (V) containing n prothrombin binding sites is

$$P_iV + P \underset{k_2}{\overset{k_1}{\rightleftharpoons}} P_{i+1}V \quad i = 0, \ldots, n-1 \tag{2}$$

The constancy of k_1 and k_2 assumes that all sites are identical and independent.

The rate equation for P is then

$$\frac{d[P]}{dt} = -k_1[P]\sum_{i=0}^{n-1}[P_iV](n-i) + k_2\sum_{i=1}^{n}[P_iV]i = -k_1[P](nV_0 - P_0 + [P]) + k_2(P_0 - [P]) \tag{3}$$

where P_0 and V_0 are the total concentrations of prothrombin and vesicle after mixing. In this latter expression both k_1 and k_2 are expressed per binding site (as opposed to per vesicle).

For the on-rate experiments, where prothrombin is mixed with phospholipid to form the P_iV complex, the analytical solution to eq 3 is

$$[P] = \frac{1}{2k_1}\left(b + q^{1/2}\frac{1 + ue^{-q^{1/2}t}}{1 - ue^{-q^{1/2}t}}\right) \tag{4a}$$

where $u = (-2k_1P_0 + b + q^{1/2})/(-2k_1P_0 + b - q^{1/2})$, $a = k_2P_0$, $b = -k_1(nV_0 - P_0) - k_2$, and $q = b^2 + 4ak_1$.

For off-rate experiments, where the P_iV complex is diluted 1:1 with buffer solution, the solution is the same as eq 4a, except that P_0 in term u is replaced by P_{eq}, the free prothrombin concentration immediately after mixing:

$$u = (-2k_1P_{eq} + b + q^{1/2})/(-2k_1P_{eq} + b - q^{1/2}) \tag{4b}$$

where $P_{eq} = (b' + q'^{1/2})/4k_1$, $a' = 2k_2P_0$, $b' = -2k_1(nV_0 - P_0) - k_2$, and $q' = b'^2 + 4a'k_1$. For dilution experiments (eq 4b) each term containing P_0 or V_0 contains a 2-fold multiplier to correct for the dilution factor.

Since the change in scattering intensity (ΔI) is used to monitor the reaction, a connection between the observed ΔI and [P] is needed. The equation derived below defines such a relationship. Let $\bar{\nu}(t)$ be the average number of protein molecules bound to a vesicle at a time t; that is

$$\bar{\nu}(t) = (P_0 - [P])/V_0 \tag{5}$$

and ignoring minor differences due to the second virial coefficient

$$I = \beta[M_{r\bar{\nu}}^2(\partial n/\partial c)_{\bar{\nu}}^2V_0 + M_{rp}^2(\partial n/\partial c)_p^2(P_0 - \bar{\nu}V_0)] \tag{6}$$

where I is the scattering intensity, β is an instrumental proportionality constant, $M_{r\bar{\nu}}$ is the average molecular weight of the protein vesicle complex, $(\partial n/\partial c)_{\bar{\nu}}$ is the average refractive index increment of the protein vesicle complex, M_{rp} is the molecular weight of prothrombin, and $(\partial n/\partial c)_p$ is the refractive index increment of prothrombin.

If we take $(\partial n/\partial c)_{\bar{\nu}}$ to be weight averaged, i.e.

$$(\partial n/\partial c)_{\bar{\nu}} = [M_{rv}(\partial n/\partial c)_v + \bar{\nu}M_{rp}(\partial n/\partial c)_p]/M_{r\bar{\nu}} \tag{7}$$

eq 6 becomes

$$I = \beta[M_{rv}(\partial n/\partial c)_v + \bar{\nu}M_{rp}(\partial n/\partial c)_p]^2V_0 + M_{rp}^2(P_0 - \bar{\nu}V_0)(\partial n/\partial c)_p^2 = \beta(I_0 + A\bar{\nu}V_0 + B\bar{\nu}^2V_0)$$

or

$$\Delta I(t) = I(t) - I(t_0) = \beta V_0B[(A/B)[\bar{\nu}(t) - \bar{\nu}(t_0)] + \bar{\nu}^2(t) - \bar{\nu}^2(t_0)] \tag{8}$$

where t_0 is the dead time of the stopped-flow equipment, M_{rv} is the molecular weight of the vesicles, $(\partial n/\partial c)_v$ is the refractive index increment of the vesicles, $I_0 = M_{rv}^2(\partial n/\partial c)_v^2V_0 + M_{rp}^2(\partial n/\partial c)_p^2P_0$ is the scattering intensity before reaction, $B = M_{rp}^2(\partial n/\partial c)_p^2$, and $A = 2M_{rv}M_{rp}(\partial n/\partial c)_v(\partial n/\partial c)_p - B$.

Equation 8 describes the rate of change in light scattering intensity as the molecular weight of the vesicles changes after mixing the samples. This analysis is based on light scattering intensity changes starting at t_0, the first observed signal from the stopped-flow apparatus. The length of the dead time for the stopped flow (t_0) had virtually no effect on this analysis when the interaction conforms to the simple bimolecular process given in eq 2. The method of fitting rate parameters to the stopped-flow data was based on internal changes in light scattering intensity (or curve shape) without reference to the absolute light scattering intensity. As shown below, this analysis establishes the relationship of the rate constants but not their absolute values. Determination of the unique rate constants requires knowledge obtained from equilibrium light scattering measurements. While these values can be obtained from the stopped-flow apparatus described here, it was more accurate and convenient to measure actual intensity changes separately by the procedure given above (eq 1; Nelsestuen & Lim, 1977).

A modified expression was used to measure dissociation in the presence of chelating agents. When a solution of P–V complexes is mixed with a chelating agent that removes the divalent cations essential for binding, the dissociation reaction becomes irreversible. If we assume that all sites are identical and independent, a first-order rate equation can be written as

$$\frac{d[P]}{dt} = +k_{off}\sum_i[P_iV]i = -k_{off}(P - P_0) \tag{9}$$

The solution to (9) is simply

$$[P] = P_0(1 - e^{-k_{off}t}) \tag{10}$$

where P_0 is the total protein concentration.

Equation 10 is used, in conjunction with eq 5 and 8, to calculate the theoretical decay curves in the data fitting process. EGTA was used as the chelating agent because it binds calcium much more tightly (log K_a = 10.7) than magnesium (log K_a = 5.4) (Williams, 1979). Thus it is possible to selectively remove calcium, which is essential to the binding of prothrombin to membrane.

Experimental data were compared visually on a computer graphic display terminal with theoretical curves generated according to eq 4, 5, and 8 for various trial values of k_1, k_2,

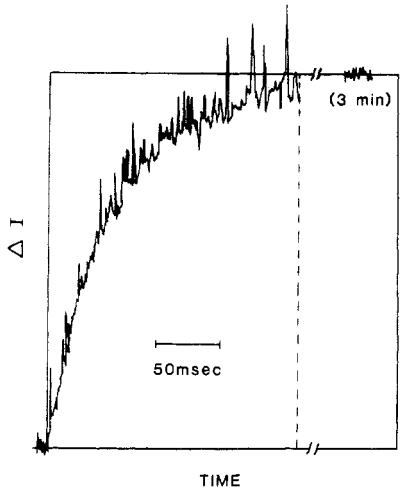

FIGURE 2: Chart tracing of the light scattering intensity when prothrombin and phospholipid vesicles are mixed. The two syringes contained (a) 300 μg of phospholipid vesicles (PS/PC, 20/80) and (b) 400 μg of prothrombin. Both solutions contained 3 mM $CaCl_2$. The intensity from the solution at full equilibrium (3 min) is also shown.

n, and t_0. Repetitive analyses of the same samples showed low variation (<10% total data range) in the rate constants obtained. Comparison studies that utilized the same preparations of protein and phospholipid (such as temperature changes) should be precise within this error limit. Independent analyses utilized different protein and phospholipid preparations on different dates. For prothrombin binding to PS/PC (20/80) at 3 mM calcium and 10 °C, such independent analyses gave a total data range of ±15% and a standard deviation of ±10% (n = 5). This is the approximate error range anticipated from uncertainties in protein and phospholipid quantitation. Data interpretations are within these error limits.

Results

Forward Rate Analysis. Figure 2 shows a chart tracing of light scattering intensity from the stopped-flow apparatus when prothrombin was mixed with phospholipid vesicles under the conditions given. Figure 3 shows comparisons of experimental data with curves generated according to eq 4, 5, and 8. The data points were taken from smooth curves drawn through the raw data (cf. Figure 2). The solid lines correspond to the theoretical curves. The observed fit to the curve shape indicated that the simple reaction model (eq 2) adequately described prothrombin–membrane interaction under these conditions. This model is characterized by single forward and reverse rate constants and noninteracting protein binding sites on the phospholipid vesicle. The rate constants in Figure 3A agreed reasonably well with the experimental data obtained over a 4-fold range in protein concentration and a 2-fold range in phospholipid concentration (see Figure 4). A single experiment run at lower phospholipid concentration (38 μg/mL) also conformed to these kinetic parameters. The small deviation (Figure 4) from total agreement with the theoretical curves consisted of a slow approach to final equilibrium. This deviation, when observed, was not considered sufficient to warrant further refinement of the kinetic model for prothrombin–membrane interaction.

The method of rate analysis described here did not determine unique values of k_1 and k_2. It was apparent that more than one set of kinetic parameters fit the rate data (compare parts A and B of Figure 3). For example, the rate data were consistent with parameters of $k_1 = 1.0 \times 10^7$ $M^{-1}\cdot s^{-1}$, $k_2 = 2$ s^{-1}, and $n = 70$ (Figure 3A) but also with $k_1 = 6 \times 10^6$ $M^{-1}\cdot s^{-1}$, $k_2 = 6$ s^{-1}, and $n = 70$ (Figure 3B).

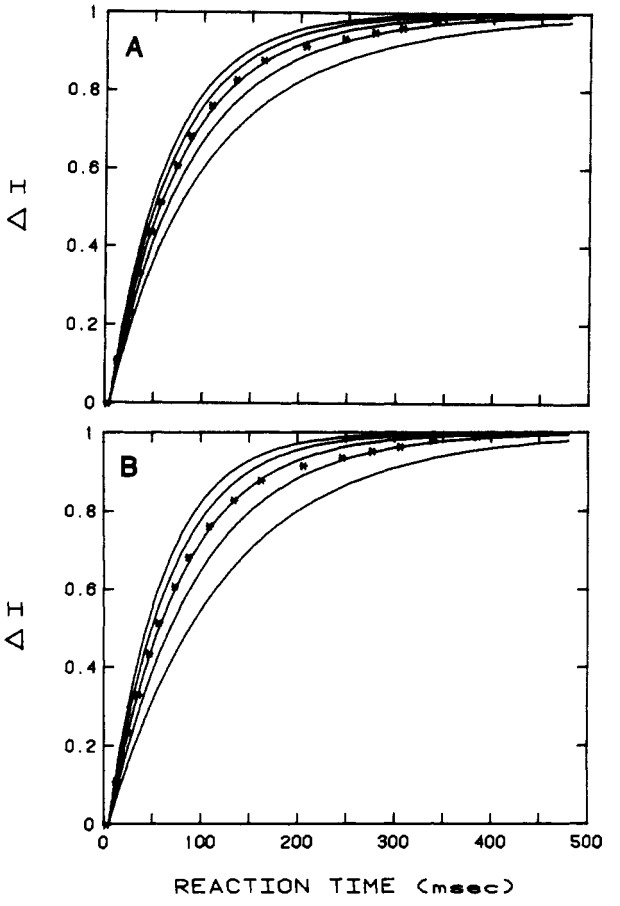

FIGURE 3: Fitting of experimental data with theoretical curves. Points from stopped-flow tracing (similar to Figure 1) are shown along with theoretical curves anticipated for trial rate parameters. The prothrombin concentration (PS/PC, 20/80) after mixing was 50 μg/mL, and the phospholipid concentration after mixing was 75 μg/mL (3 mM final Ca^{2+}). The curves shown are for the rate parameters n = 70, $k_1 = 1.1 \times 10^7$ $M^{-1}\cdot s^{-1}$, and variable k_2 values. Beginning with the lowest line, the k_2 values correspond to 0, 1, 2, 3, and 4 s^{-1}. Part B shows curve fitting to the same experimental data for the kinetic parameters n = 70, $k_1 = 6 \times 10^6$ $M^{-1}\cdot s^{-1}$, and k_2 = 2, 4, 6, 8, and 10 s^{-1}.

During these studies much broader variations in the rate parameters were tested. It appeared that stipulation of any two parameters would still allow fitting to the experimental result by variation of the third parameter. Variations in n and k_1 were always directly compensating as expected from eq 3. Fortunately, the variations of k_1 and k_2 necessary to fit the experimental curves were in opposite directions, resulting in a very large effect on the equilibrium constant and on the absolute light scattering intensity change at equilibrium. In the example given above, a 40% reduction in k_1 required a 5-fold change in K_D to fit the rate data. Therefore, k_1 and k_2 can be determined accurately if the equilibrium constant is known within even substantial error limits.

This kinetic analysis by itself did set an upper limit for the value of k_1. This was obtained when k_2 was set to zero. The upper limit for k_1 obtained from the data in Figure 3 was 1.4×10^7 $M^{-1}\cdot s^{-1}$.

Equilibrium Prothrombin–Membrane Binding Measurements. Demonstration that the apparent dissociation constant was constant at various phospholipid concentrations constituted a test for the validity of equilibrium binding measurements. Binding experiments are shown over a 12-fold range in phospholipid concentration (Figure 5). These include the extreme conditions under which reliable measurement of free

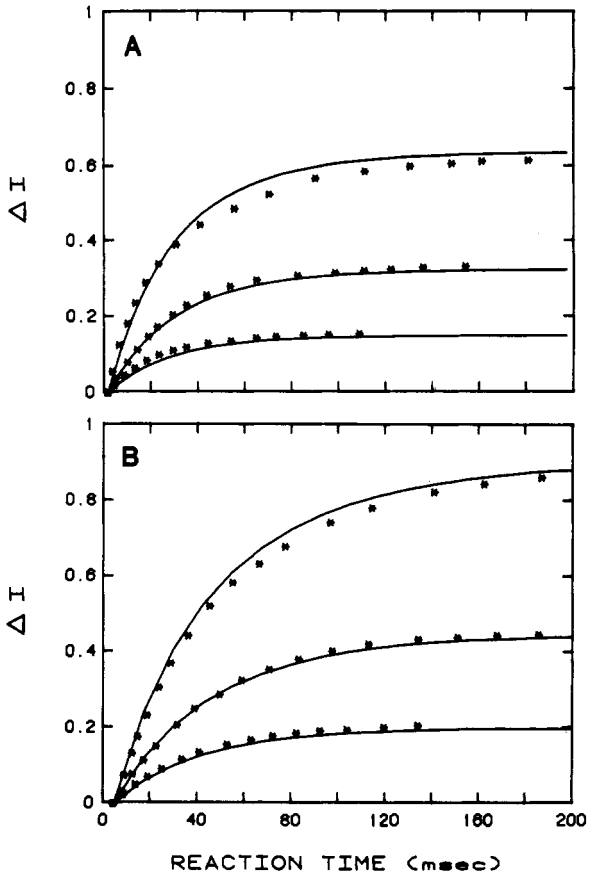

FIGURE 4: Curve fitting for varying prothrombin and phospholipid concentrations. Experimental data points were taken from the stopped-flow tracings as described in Figure 3. The magnitude of intensity change also conforms to experimental observation. The theoretical curves (solid lines) must therefore conform to both curve shape and relative intensity change. The theoretical rate parameters for all curves are $n = 70$, $k_1 = 1.1 \times 10^7$ $M^{-1}\cdot s^{-1}$, and $k_2 = 2$ s^{-1}. In part A the phospholipid concentration (PS/PC, 20/80) after mixing was 75 μg/mL, and the prothrombin concentrations were 25, 50, and 100 μg/mL (beginning with the bottom curve). In part B the phospholipid concentration after mixing was 150 μg/mL, and the prothrombin concentrations were 50, 100, and 200 μg/mL (3 mM final Ca^{2+}).

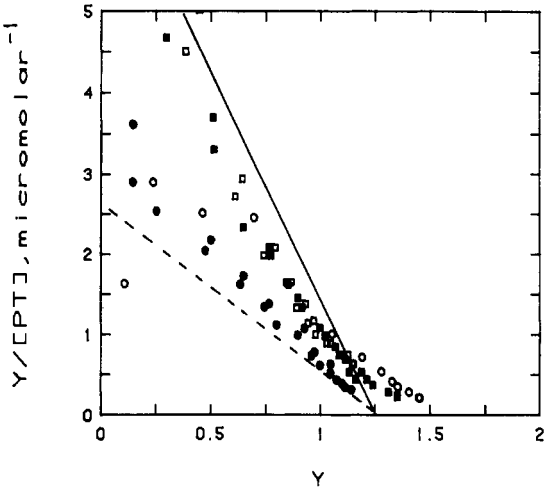

FIGURE 5: Equilibrium prothrombin–membrane binding measurements. Free and membrane-bound prothrombins were measured by the technique described under Materials and Methods at 3 mM calcium. Phospholipid concentrations (PS/PC, 20/80) used include 12 (■), 24 (□), 48 (●), and 142 μg/mL (○). Duplicate titrations were conducted on succeeding days with different protein preparations. The term $\bar{y}$ is the grams of prothrombin bound per gram of phospholipid. The binding curves drawn are the theoretical binding curves for two sets of rate parameters: the solid line represents $n = 70$, $k_1 = 1.1 \times 10^7$ $M^{-1}\cdot s^{-1}$, and $k_2 = 2$ s^{-1}; the dashed line represents $n = 70$, $k_1 = 9 \times 10^6$ $M^{-1}\cdot s^{-1}$, and $k_2 = 4$ s^{-1}. Both sets of rate parameters satisfy the kinetic data (Figure 3).

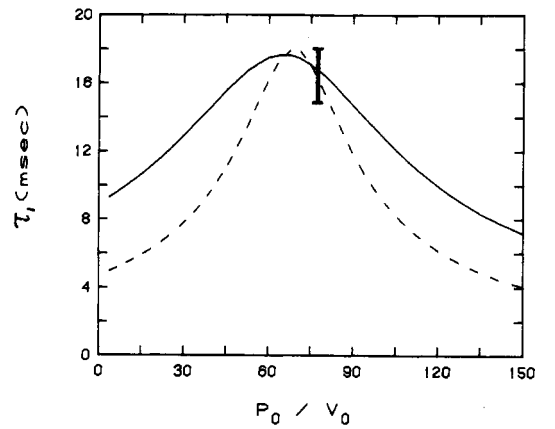

FIGURE 6: Rates for approach to equilibrium after sample dilution. Theoretical τ_1 values are shown for a solution of 360 μg of phospholipid and 500 μg of prothrombin/mL. The theoretical τ_1 values for the two sets of kinetic parameters are given. The curves represent rate parameters of $n = 70$ (in both cases), $k_1 = 6 \times 10^6$ $M^{-1}\cdot s^{-1}$, and $k_2 = 6$ $s^{-1}\cdot$vesicle^{-1} (solid line); $k_1 = 1.1 \times 10^7$ $M^{-1}\cdot s^{-1}$ and $k_2 = 2$ s^{-1} (dashed line). The experimentally determined point is shown. The error bars indicate signal noise.

and bound prothrombin can easily be made by this method. For example, lower concentrations of phospholipid resulted in increased interference from dust particles and required significant corrections for light scattering from free prothrombin. Higher concentrations gave rise to errors because of the very small proportion of free protein. As seen, each concentration of phospholipid gave a nearly linear relationship indicative of a single binding constant. The intercepts of all curves indicated a vesicle capacity of about 1.3 g of prothrombin bound/g of phospholipid or 73 prothrombin molecules bound/vesicle of 4×10^6 daltons. Intercepts from these types of plots were the basis for setting the values of n reported below. The two curves shown in Figure 5 correspond to a dissociation constant for prothrombin–membrane binding of $(3 \pm 1) \times 10^{-7}$ M. This value agreed very closely to previously reported values under similar conditions (Nelsestuen & Broderius, 1977; Resnick & Nelsestuen, 1980).

Given the apparent maximum uncertainty in the equilibrium constant [$(3 \pm 1) \times 10^{-7}$ M^{-1}, Figure 5], the kinetic experiments provide that the value of k_1 (at $n = 70$) was within the narrow range of $(1 \pm 0.1) \times 10^7$ $M^{-1}\cdot s^{-1}$ and k_2 was 3 ± 1 s^{-1}.

Dilution Studies. Dissociation of protein from vesicles can be measured directly by dilution of preformed complexes. For off-rate dilution studies the signal change was relatively small, and the signal to noise ratio did not warrant fitting the entire curve. Therefore, the first half-time for approach to equilibrium, τ_1, was determined. When a solution containing 760 μg of phospholipid plus 1000 μg of prothrombin was mixed 1:1 with buffer in the stopped-flow apparatus, the value of τ_1 was 16 ms. A plot of theoretical τ_1 values, which fit the rate parameters estimated from the forward rate analysis, is shown in Figure 6. Agreement with experiment is good. This observation again supports the validity of the overall model for this interaction. However, approach to equilibrium after dilution once again failed to specify the unique values of k_1 and k_2. As shown in Figure 6, at least two sets of rate constants were consistent with the half-time of this dilution experiment. From the theoretical curves it is apparent that either much higher or much lower protein to phospholipid ratios should allow assignment of the correct rate constants. Un-

Table I: Prothrombin-Membrane Binding Characteristics at 10 °C

phospholipid (composition)	vesicle parameters			binding parameters at saturating calcium				theor max	collision effi-	ΔH^{+} [b]
	$D_{20,w}$ ($cm^2 \cdot s^{-1}$)	$2R_h$ (nm)	M_r	k_1 ($M^{-1} \cdot s^{-1}$)	k_2 (s^{-1})	n	K_D (M)	nk_1 ($M^{-1} \cdot s^{-1}$)[a]	ciency (%)	(kcal/mol)
PS/PC (10/90)	1.68×10^{-7}	29.6	3.5×10^6	6×10^6	4	30	7×10^{-7}	6.7×10^9	2.7	9.2
PS/PC (20/80)	1.66×10^{-7}	30.0	3.2×10^6	15×10^6	4	57	3×10^{-7}	6.7×10^9	13	6.9
PS/PC (40/60)	1.77×10^{-7}	28.0	3.7×10^6	17×10^6	5	72	3×10^{-7}	6.4×10^9	19	3.7
PG/PC (20/80)	2.08×10^{-7}	24.0	2.5×10^6	6×10^6	25	36	40×10^{-7}	6.0×10^9	3.6	
PG/PC (40/60)	2.12×10^{-7}	23.5	2.3×10^6	19×10^6	15	48	8×10^{-7}	5.9×10^9	15	
PE/PC (40/60)	1.35×10^{-7}	37.0	7.4×10^6	6×10^6	22	61	36×10^{-7}	7.4×10^9	5	
FFIII/PC[c] (25/75)			3.5×10^6	9×10^6	7.0	44	8×10^{-7}	6.7×10^9	6	

[a] nk_1 corresponds to the collisional frequency calculated from diffusion constants and Stokes radii according to Smoluckowski's theory. [b] ΔH^{+} is approximately the same for association and dissociation. [c] Folch fraction III.

fortunately, these conditions were not experimentally accessible because of the very small changes in the signal and/or short reaction times. Consequently, the dilution study provided a different approach to these studies and provided evidence supporting the model but did not establish unique values for the rate constants without use of equilibrium measurements.

Effects of Calcium. Previous studies (Nelsestuen & Lim, 1977; Dombrose et al., 1979; Resnick & Nelsestuen, 1980) on prothrombin–membrane interaction at equilibrium have shown that the equilibrium dissociation constant decreased as the calcium concentration was increased in the range 2–10 mM. There was no further change at higher Ca^{2+} concentrations. Figure 7 presents the association and dissociation rate constants obtained over this calcium concentration range. The association rate constant appeared less sensitive to calcium in this concentration range (Figure 7A) than the dissociation rate constant (Figure 7B). This was generally true for the three types of phospholipid used in this study, phosphatidylserine, phosphatidylethanolamine, and phosphatidylglycerol mixed in with phosphatidylcholine.

Different Phospholipids. Table I summarizes the binding characteristics for prothrombin interaction with various phospholipids at saturating calcium concentrations. In comparing the values in Table I, it is important to realize that different phospholipids gave vesicles of different average size. This is obvious from the average diameters determined by quasi-elastic light scattering analysis, the molecular weights determined by light scattering intensity analysis (Table I), and the elution profiles from gel filtration (Figure 8). As a result of these different vesicle sizes and diffusion constants, the theoretical collision rate between protein and vesicles (theoretical maximum for nk_1, Table I) varied somewhat. Since the forward rate constants were expressed on a binding site basis, they must be multiplied by n, the number of sites per vesicle, before comparison to the theoretical collision rate. The collision efficiency was therefore obtained by dividing the experimental value of nk_1 by the theoretical collision rate. An additional effect of the different vesicle size was that the values for n, the number of prothrombin binding sites per vesicle, cannot be directly compared; the size of the vesicle must also be considered when estimating the number of prothrombin binding sites per unit weight of phospholipid. This study did not attempt to determine the effect of vesicle size on rate parameters. Previous studies of equilibrium binding constants (Nelsestuen & Lim, 1977) indicated that the vesicle size had relatively little effect on binding affinity.

The data presented in Table I reveal several interesting aspects of prothrombin–membrane binding. For phosphatidylserine–phosphatidylcholine mixtures, the forward rate constant per binding site, or collisional efficiency, increased with the phosphatidylserine content of the membrane. This

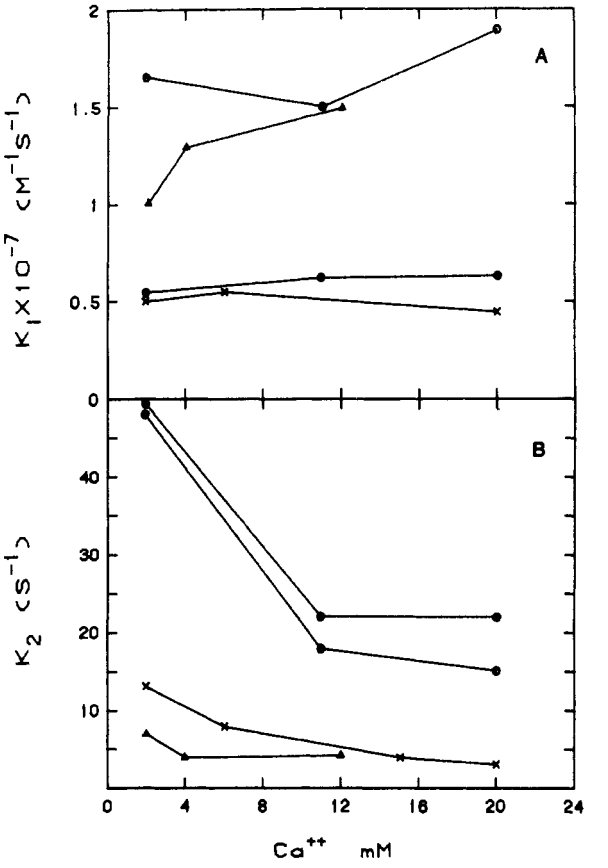

FIGURE 7: Effects of calcium concentration on forward and reverse rate constants. The prothrombin and single bilayer phospholipid concentrations used were 150–300 μg/mL before mixing in the stopped-flow apparatus. The phospholipid compositions used were as follows: PS/PC (10/90) (×); PS/PC (20/80) (▲); PG/PC (40/60) (○); PE/PC (40/60) (●).

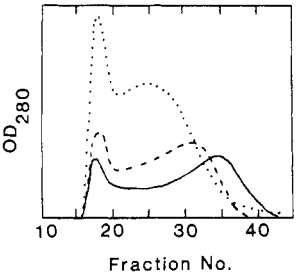

FIGURE 8: Elution profile of phospholipids from gel-filtration chromatography. The phospholipid mixtures were sonicated and chromatographed on a Sepharose 4B column (2 × 40 cm). The absorbance at 280 nm was followed to give an estimation of phospholipid concentration. The elution profiles shown are PG/PC (40/60) (—), PS/PC (20/60) (– –), and PE/PC (40/60) (···). The second half of the included peak was pooled for use in stopped-flow analysis.

suggested a cooperative effect of phosphatidylserine on the forward rate constant, i.e., that more than one phosphatidylserine residue was involved in a successful collision with prothrombin. The cooperativity was not great, however, with a 7-fold increase in collision efficiency over a 4-fold increase in phosphatidylserine content. This suggestion of cooperativity was also seen in the forward rate constants for membranes containing phosphatidylglycerol. In this case the collisional efficiency increased 4-fold when the phosphatidylglycerol content was doubled. In contrast to the forward rate constants, the dissociation rate constant (k_2) was nearly unaffected by the amount of acidic phospholipid in the membrane (Table I).

It was previously observed that prothrombin binding to phosphatidylglycerol was less tight than to phosphatidylserine (Nelsestuen & Broderius, 1977). The results in Table I indicate that this lower affinity is largely due to the dissociation rate constant which is 3–5-fold greater for the phosphatidylglycerol membranes. This analysis did not attempt to correct for the effect of asymmetric distribution of these phospholipids. Since phosphatidylglycerol partitions to the outside of small vesicles (Michaelson et al., 1973) while phosphatidylserine partitions to the inside (Berden et al., 1975), the real difference between these two phospholipids in binding prothrombin is probably more striking than these data suggest.

Membranes containing phosphatidylcholine–phosphatidylethanolamine also bind prothrombin (Table I; Nelsestuen & Broderius, 1977). The rate constants obtained with these phospholipid vesicles (Table I) provided data supporting some of the principal characteristics of prothrombin–membrane binding. Phosphatidylethanolamine partitions preferentially to the inside of these vesicles (Litman, 1974).

Kinetic analysis of prothrombin interaction with membranes containing Folch fraction III, a crude source of phosphatidylserine, was conducted to allow comparisons to enzymatic rate data (Nesheim et al., 1979). As seen, the binding parameters showed small differences when compared to membranes containing approximately similar amounts of phosphatidylserine.

Dissociation Rates Obtained by Removing Calcium. Since prothrombin–membrane interaction is calcium dependent, removal of calcium causes dissociation of the complex. Kinetic analysis of this type of dissociation can reveal characteristics of calcium exchange in the complex. Stopped-flow experiments in which prothrombin–phospholipid complexes (3 mM Ca^{2+}) were mixed with 10 mM EGTA showed rapid dissociation of the complex, consistent with a rate constant of greater than 100 s^{-1} (experiment 1, Table II). Since this was much greater than k_2, we concluded that an essential population of calcium in the complex was in rapid exchange; removal of this calcium caused immediate dissociation of prothrombin from the membrane. A similar result was obtained with a 10% excess of EGTA (experiment 2, Table II).

Previous studies have shown the participation of two pools of metal ions in prothrombin–membrane binding: the first causes a protein conformational change while the second is required in some other role for forming the prothrombin–membrane complex (Nelsestuen et al., 1976). Magnesium and manganese function in the first role but not in the second. Table II shows experiments where excess magnesium was included. Similar results were obtained when 1 mM manganese was substituted for the magnesium. In these experiments the EGTA added was sufficient to chelate the calcium, but excess magnesium remains to satisfy the protein conformation requirements. A stopped-flow tracing of dissociation

Table II: Dissociation Rates Obtained with EGTA

expt	soln composition[a]	k_{off} (s^{-1})[b]	k_2 (s^{-1})[c]
1	(A) PS/PC (20/80), prothrombin, 3 mM Ca^{2+}	≥100	
	(B) 12 mM EGTA		
2	(A) PS/PC (20/80), prothrombin, 3 mM Ca^{2+}	≥100	
	(B) 3.3 mM EGTA		
3	(A) PS/PC (20/80), prothrombin, 3 mM Ca^{2+}, 4 mM Mg^{2+}	15	4
	(B) 3.3 mM EGTA		
4	(A) PS/PC (40/60), prothrombin, 3 mM Ca^{2+}, 4 mM Mg^{2+}	3	5
	(B) 3.3 mM EGTA		
5	(A) PS/PC (10/90), prothrombin, 10 mM Ca^{2+}, 6 mM Mg^{2+}	40	4
	(B) 12 mM EGTA		

[a] Solution A was mixed with solution B in the stopped-flow apparatus. Protein and phospholipid concentrations were 150–300 μg/mL each before mixing. [b] k_{off} represents the dissociation rate constant obtained from these experiments by the methods described. [c] k_2 is the dissociation rate constant obtained from kinetic analysis (Table I).

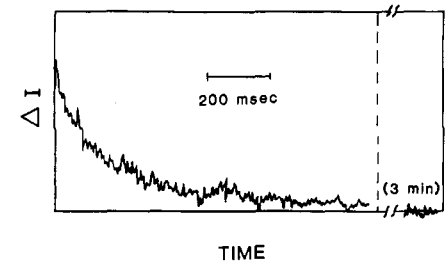

FIGURE 9: EGTA-induced dissociation of prothrombin from phospholipid vesicles. One syringe of the stopped-flow apparatus contained phospholipid (150 μg/mL of PS/PC, 40/60), prothrombin (120 μg/mL), 3 mM calcium, and 4 mM magnesium. The second syringe contained 3.3 mM EGTA. The light scattering intensity change after mixing is shown. The intensity at equilibrium (3 min) is also given. For estimation of the dissociation rate constants, points taken from a smooth line drawn through this curve were compared to theoretical curves.

observed under these conditions is illustrated in Figure 9. The rate constants (k_{off}) estimated from these experiments are given in Table II. In all cases, the rate constants in the presence of excess magnesium ion indicated a slower dissociation than in its absence. This indicated that a second group of essential calcium ions dissociated more slowly. This dissociation displays first-order kinetics over its entire course.

Effects of the Method of Calcium Addition. The results in Table III illustrate different methods of adding calcium to form the prothrombin–membrane complex. Preequilibration of phospholipid with calcium had no significant effect on the rate of prothrombin–membrane binding (compare experiments 1 and 2, Table III). The rate for calcium interaction with the phospholipid is therefore rapid on the time scale of protein–membrane interaction.

A calcium-dependent prothrombin conformational change, which must precede membrane binding, occurs at two clearly distinguishable rates (Nelsestuen, 1976). About 25% of the protein molecules undergo a rapid conformational change while 75% undergo the change with a rate constant of 0.000 46 s^{-1} at 10 °C (Nelsestuen, 1976). Marsh et al. (1979) have attributed the two populations of prothrombin to a *cis–trans*-proline equilibrium in the apoprotein. Protein molecules with the correct proline conformation bind calcium rapidly and undergo a rapid conformational change, which allows mem-

Table III: Effects of Ca^{2+} Addition and Ionic Strength on Rate Constants

expt	soln composition[a]	k_1 ($M^{-1}\cdot s^{-1}$)	k_2 (s^{-1})
1	(A) PS/PC (300 μg/mL), 4 mM Ca^{2+} (B) prothrombin (300 μg/mL), 4 mM Ca^{2+}	8.4×10^6	2.5
2	(A) PS/PC (300 μg/mL), 0 mM Ca^{2+} (B) prothrombin (300 μg/mL), 8 mM Ca^{2+}	10×10^6	3.0
3	(A) PS/PC (140 μg/mL), 2 mM Ca^{2+} (B) prothrombin (250 μg/mL), 2 mM Ca^{2+}	6.2×10^6	3.7
4	(A) PS/PC (140 μg/mL), 4 mM Ca^{2+} (B) prothrombin (1000 μg/mL), 0 mM Ca^{2+}	6×10^6	3.6
5	(A) PS/PC (300 μg/mL), 12 mM Ca^{2+}, 0 M NaCl[b] (B) prothrombin (300 μg/mL), 12 mM Ca^{2+}, 0 M NaCl	8.2×10^6	2.5
6	(A) PS/PC (300 μg/mL), 12 mM Ca^{2+}, 0.4 M NaCl[c] (B) prothrombin (300 μg/mL), 12 mM Ca^{2+}, 0.4 M NaCl	4.3×10^6	2.1

[a] Solution A was mixed 1:1 with solution B in the stopped-flow apparatus. Unless indicated all solutions contained 0.1 M NaCl. Experiments for direct comparison were run on the same day with the same preparations. [b] The capacity was 70 prothrombin binding sites/vesicle of 4×10^6 daltons. [c] The capacity was 35 prothrombin binding sites/vesicle of 4×10^6 daltons.

brane binding. Protein molecules with the incorrect proline conformation must undergo the slow *cis–trans*-proline isomerization before the conformation change and membrane binding occur. In light of this model, the relative rate of the former process was investigated by experiments 3 and 4 (Table III). Experiment 3 contained prothrombin preequilibrated with calcium so all molecules were in the correct proline conformation. Experiment 4 contained 4 times as much apoprothrombin. The concentration of protein molecules with the correct proline conformation should be similar in these two experiments. The rates of prothrombin–membrane binding were similar in these two experiments, indicating that the calcium-induced conformational change occurring in molecules with the correct proline conformation was rapid on this time scale. *cis–trans*-Proline isomerization is so slow that it did not contribute to binding on the time scale of the stopped flow.

Effects of Ionic Strength. Resnick & Nelsestuen (1980) reported that, at saturating calcium, the binding affinity of prothrombin for 20% phosphatidylserine was relatively unaffected by ionic strength but the number of binding sites per unit of phospholipid decreased at higher ionic strength. This conclusion was substantiated by kinetic analysis of prothrombin–membrane binding at different ionic strengths (Table III, experiments 5 and 6). The k_1 values are directly comparable since they are expressed on a protein binding site basis. It is apparent that ionic strength had a relatively minor effect on the rate constant for prothrombin–membrane association when calcium was saturating.

Anomalous Binding at High Protein Concentration. Due to the advantages of increased signal intensity, initial experiments in this study were run at much higher protein and phospholipid concentrations. An example of the rate data obtained under these conditions is shown in Figure 10. Several observations suggest a binding interaction with complex kinetic parameters. First of all, the simple bimolecular interaction

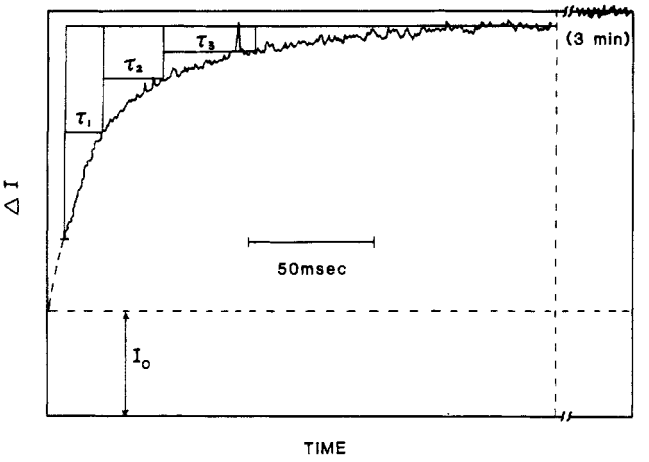

FIGURE 10: Stopped-flow tracing at high protein concentration. The phospholipid concentration after mixing was 580 μg/mL, and the protein concentration was 0.9 mg/mL. The intensity of light scattering from the phospholipid vesicles and prothrombin before binding occurs is indicated by I_0. Reaction half-times (τ_1, τ_2, and τ_3) are indicated. Light scattering intensity at equilibrium (3 min) is also shown.

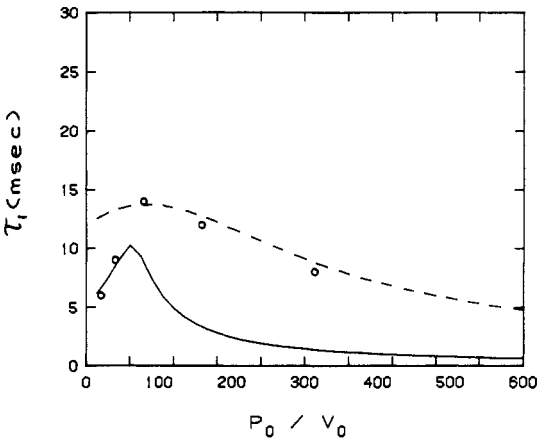

FIGURE 11: Experimental observations at high protein concentration. The τ_1 values obtained as in Figure 7 are plotted as a function of prothrombin to phospholipid (mole/mole) ratio. The phospholipid concentration used was the same as shown in Figure 7. The curves are theoretical τ_1 values for different sets of rate constants. The solid line is for $n = 70$, $k_1 = 1.1 \times 10^7$ $M^{-1}\cdot s^{-1}$, and $k_2 = 2$ s^{-1}, and the dashed line is for $n = 150$, $k_1 = 1.3 \times 10^6$ $M^{-1}\cdot s^{-1}$, and $k_2 = 15$ s^{-1}.

given in eq 2 predicts that the half-times (τ) of the binding interaction should be approximately constant over the entire binding curve. Figure 10 shows that the second half-time, τ_2, is 30–50% longer than τ_1. These half-time measurements are based on light scattering intensity and should be corrected according to eq 8. Nevertheless, rate parameters obtained when measured light scattering intensity was used directly to analyze prothrombin–membrane binding deviated only 10–20% from those obtained by corrected analysis. Consequently, direct analysis of intensity measurements gives a reasonably accurate estimation of the kinetics of binding.

A second anomaly associated with the use of high protein and phospholipid concentrations was that the rate constants obtained in the studies given above ($k_1 = 1 \times 10^7$ $M^{-1}\cdot s^{-1}$ and $k_2 = 3$ s^{-1}) predict a much more rapid interaction (τ_1 of about 2 ms) than was observed (Figure 10). It is therefore clear that, under the conditions used in Figure 10, the rate constants varied with the degree of membrane saturation and the rate constants were quite different from those observed in more dilute solution.

Figure 11 shows a plot of first half-reaction times (τ_1) for prothrombin–membrane binding as a function of prothrombin

to phospholipid concentration ratios when the total phospholipid concentration was high (800 μg/mL). No single combination of rate parameters was consistent with all the results. The solid line shows the τ_1 values expected for the rate constants given above (n = 70; $k_1 = 1.1 \times 10^7$ $M^{-1}\cdot s^{-1}$; $k_2 = 2$ s^{-1}). As seen, data obtained below 70 protein molecules/vesicle correlate well with this theoretical curve. When the protein concentration per vesicle exceeded the number of binding sites, however, the rate was much slower than predicted by these rate constants. Since the phospholipid concentration was high, excess prothrombin resulted in high concentrations of free protein. For example, at 300 prothrombin molecules/vesicle (Figure 12) the total prothrombin concentration was 3.3 mg/mL. Anomalous data were therefore observed when the free prothrombin concentration became high.

One explanation for the deviation from ideality at high protein concentrations was the existence of low-affinity binding sites on the phospholipid vesicle. The dashed line in Figure 11 corresponds to the expected τ_1 values for the set of rate parameters: n = 150, $k_1 = 1.3 \times 10^6$ $M^{-1}\cdot s^{-1}$, and $k_2 = 15$ s^{-1}. These correspond to a dissociation constant of 11 μM. These values were obtained from analysis of τ_1 only. Analysis of τ_2 or τ_3 would give different rate parameters with even higher dissociation constants.

Discussion

The stopped-flow light scattering technique used in this study should have general applicability to systems involving protein–vesicle interactions. Most of the potential errors associated with application of this technique did not apply to comparison studies. Consequently, conclusions based on data comparisons are more precise than the absolute values for the rate constants. Analysis of prothrombin–membrane binding by this technique provided insight into the dynamic aspects of this interaction. Under conditions which are likely to be important physiologically (≤3 μM prothrombin and membranes of about 20% acidic phospholipid), this association conformed reasonably well to a simple bimolecular interaction between protein and binding sites on the phospholipid vesicles. The small deviations from ideal behavior were considered insufficient to warrant further refinement of this model for protein–membrane binding.

The maximum forward rate constant for a diffusionally controlled process involving spherical particles can be estimated from the collisional frequency according to Smoluchowski's theory (Smoluchowski, 1915, 1917):

$$k = 4\pi N_{AV}(D_V + D_P)(R_V + R_P)/1000$$

where D and R are the diffusional coefficient and Stokes radius, respectively, and the subscripts V and P stand for vesicles and prothrombin molecules. In the present example, the diffusion coefficient and the radius of the protein–vesicle complex change as the reaction proceeds. Over the entire binding curve these changes are less than 2-fold. We estimate that direct application of Smoluchowski's theory to this system should introduce only about a 20% error from this source. This error should not apply to comparison studies. A good first approximation of collisional efficiency should be obtained. From the diffusion constant and Stokes radius of prothrombin [$D_{20,w} = 4.8 \times 10^7$ cm^2/s; R = 4.9 nm (Nelsestuen et al., 1981)] and the 20% phosphatidylserine vesicles used ($D_{20,w} = 1.73 \times 10^{-7}$ cm^2/s; R = 15 nm), the maximum forward rate constant based on collisional frequency at 10 °C is 6.7×10^9 $M^{-1}\cdot s^{-1}$. The rate constants obtained here are expressed per protein binding site and must be multiplied by n, the number of sites per vesicle, for comparison to the maximum rate constant. Thus, the experimentally obtained forward rate constant for 20% phosphatidylserine vesicles can be expressed as 7×10^8 $M^{-1}\cdot s^{-1}\cdot vesicle^{-1}$, which corresponds to about a 10% collisional efficiency (Table I).

The association rate constant and collisional efficiency showed some cooperativity with respect to acidic phospholipid content in the membrane. One interpretation of this result is that simultaneous interaction of prothrombin with more than one phosphatidylserine residue in the membrane is necessary for a successful collision. Other explanations for this behavior are also possible. For example, higher acidic phospholipid composition may improve the spatial organization of the phospholipids in the membrane.

In contrast, when calcium was saturating, the dissociation rate constant was relatively insensitive to the overall charge density of the membrane. The most likely explanation for this observation is that bound prothrombin interacts with a similar number of acidic phospholipid residues regardless of the membrane composition. This suggests a discrete cluster of acidic phospholipids bound to the protein and is consistent with studies on prothrombin-induced lateral phase separation in mixed phospholipid membranes (Mayer & Nelsestuen, 1981).

Studies at different ionic strengths demonstrated that sodium chloride had relatively little effect on rate constants for binding of calcium-saturated prothrombin to calcium-saturated phospholipid (Table III; Resnick & Nelsestuen, 1980). This suggests that the final binding interaction does not involve a charge–charge recognition. Sodium chloride reduced the number of protein binding sites on the membrane, and the data are consistent with a situation where sodium effectively masked some of the acidic phospholipid residues. For example, the binding constants and number of sites per vesicle of 20% phosphatidylserine at 0.4 M NaCl (Table III) were similar to these parameters for membranes of 10% phosphatidylserine at 0.1 M NaCl (Table I). This effect may be related to actual sodium ion binding to phosphatidylserine, which occurs in this concentration range (Hauser et al., 1976). These effects did not appear to be strictly competitive with calcium ion since the latter was saturating under both conditions. Further understanding of sodium and calcium ion interaction with phospholipids appears necessary to interpret these results effectively.

The maximum collisional efficiency between prothrombin and phospholipids studied was estimated to be 20%. That is, one in five protein–membrane collisions resulted in binding. The membrane binding region of prothrombin, fragment 1 (residues 1–156 of prothrombin, Magnusson et al., 1975), contains only about 30% of the amino acid residues in prothrombin. It is therefore apparent that collision between certain regions of prothrombin and the phospholipid cannot be successful. The data (Table I) suggested that a 20% collisional efficiency approached the maximum value. This was supported by a small relative increase in collisional efficiencies for membranes of 20 and 40% phosphatidylserine (Table I). That the activation energy approached that of a diffusionally controlled process (Figure 12A) for membranes of 40% phosphatidylserine also supports the idea that a maximum collisional efficiency was approached. Investigations at higher phosphatidylserine composition were not possible due to calcium-induced changes in the light scattering properties of these vesicles (Nelsestuen & Broderius, 1977).

Rates of prothrombin–membrane dissociation after removal of calcium by EGTA chelation revealed that a population of essential metal ions was in rapid exchange even when the protein was bound to the membrane. This population can

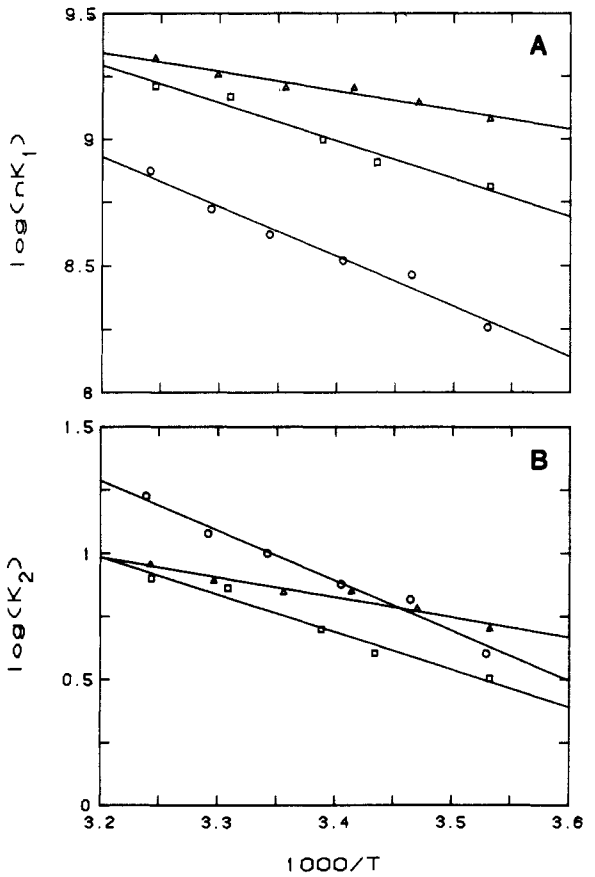

FIGURE 12: Estimation of the activation energy for prothrombin–membrane binding. Part A shows an Arrhenius plot of the association rate constant estimated for prothrombin binding to PS/PC vesicles of content 10/90 (○), 20/80 (□), and 40/60 (△). Part B gives the dissociation rate constants. These values were obtained by using a temperature-insensitive dissociation constant for each phospholipid.

apparently be replaced by magnesium or manganese. This ion specificity suggests that the rapidly exchanging pool corresponds to metal ions involved in maintaining the appropriate protein conformation (Nelsestuen et al., 1976). A second pool of metal ions, apparently specific for calcium, was in slower exchange and, in some instances, exchanged only at the rate of prothrombin dissociation from the membrane. One interpretation of these findings is that the second pool of calcium ions is at least partially trapped in the prothrombin–membrane complex. These ions may be involved in bridging between protein and phospholipid, possibly by coordination to both entities (Lim et al., 1977).

Finally, the rate of prothrombin–membrane interaction can provide insight into the kinetic mechanism of prothrombin interaction with the prothrombinase complex. An initial question is how the binding of prothrombin and the prothrombinase proteins (factor Xa–factor Va) to the membrane affects the rate of prothrombin to thrombin conversion. Without presenting actual calculations, it is clear that the rate of association and dissociation of prothrombin from an entire vesicle is much greater than reported enzymatic rate constants (Nesheim et al., 1979; Rosing et al., 1980). That is, given 1 prothrombinase complex/phospholipid vesicle, the association and dissociation of prothrombin from the vesicle are faster than enzyme catalysis by the complex. In fact, the association of prothrombin with a single binding site on the membrane (k_1 = 3 × 10^7 $M^{-1}\cdot s^{-1}$ at 37 °C) is reasonably close to the rate constants for the prothrombinase complex, 3.5 × 10^7 $M^{-1}\cdot s^{-1}$ (Nesheim et al., 1979) and 1.6 × 10^8 $M^{-1}\cdot s^{-1}$ (Rosing et al., 1980), calculated from reported K_{cat} and K_m values. The dissociation rate constant for prothrombin–membrane binding at 37 °C (10–20 s^{-1} or larger) is also similar to the reported k_{cat} values. From these data it appears possible that a single prothrombinase complex requires a relatively small membrane surface area for binding substrate and the enzymatic velocity at low substrate concentrations may be limited by successful collisions at that site of the complex. Further studies are obviously necessary for understanding of this complex enzymatic system.

At high free-prothrombin concentrations prothrombin–membrane binding characteristics no longer conform to a single class of noninteracting binding sites. Under these conditions the results suggest that the sites show variable rate constants at different degrees of phospholipid saturation. This complex binding behavior does not appear to be explained simply by a second class of low-affinity binding sites. The kinetics of binding (see Figure 6) suggested that the entire course of binding was much slower than expected. While there may be several explanations for this behavior, we have not attempted to elucidate its basis. These anomalous binding results were significant when the protein concentration became much higher than physiological. The analyzed kinetic binding studies were generally conducted under conditions well below saturation of the protein sites on the membrane (e.g., Figures 3 and 4).

The overall results of this kinetic analysis lend further support to the general view of prothrombin interaction with phospholipid membranes in a very peripheral manner. Identification of the functional groups involved in protein–membrane contact will require further study.

References

Berden, J. A., Barker, R. W., & Radda, G. A. (1975) *Biochim. Biophys. Acta 375*, 186–208.

Bloomfield, V. A., & Lim, T. K. (1978) *Methods Enzymol. 48*, 415–494.

Bunn, C. R., Keele, B. B., Jr., & Elkan, G. H. (1969) *J. Chromatogr. 45*, 326.

Dombrose, F. A., Gitel, S. N., Zawalich, K., & Jackson, C. M. (1979) *J. Biol. Chem. 254*, 5027–5040.

Hanahan, D. J., Barton, P. G., & Cox, A. (1969) in *Human Blood Coagulation: Proceedings of the Boerhaave Course for Postgraduate Medical Education, Leiden, 1968* (Hemker, H. C., et al., Eds.) Springer-Verlag, New York.

Hauser, H., Drake, A., & Phillips, M. C. (1976) *Eur. J. Biochem. 62*, 335–344.

Hax, W. M. A., & Guerts van Kessel, W. S. M. (1977) *J. Chromatogr. 142*, 735–741.

Huang, C. (1969) *Biochemistry 8*, 344–352.

Jackson, C. M., & Nemerson, Y. (1980) *Annu. Rev. Biochem. 49*, 727–766.

Liddle, P. F., Jacobs, D. J., & Kellett, G. L. (1977) *Anal. Biochem. 79*, 276–290.

Lim, T. K., Bloomfield, V. A., & Nelsestuen, G. L. (1977) *Biochemistry 16*, 4177–4181.

Litman, B. J. (1974) *Biochemistry 13*, 2844–2852.

Magnusson, S., Petersen, T. E., Sottrup-Jensen, L., & Claeys, M. (1975) in *Proteases and Biological Control* (Reich, E., Rifkin, D. B., & Shaw, E., Eds.) p 123, Cold Spring Harbor Laboratory, Cold Spring Harbor, NY.

Marsh, H. C., Scott, M. E., Hiskey, R. G., & Koehler, K. A. (1979) *Biochem. J. 183*, 513–517.

Mayer, L. D., & Nelsestuen, G. L. (1981) *Biochemistry 20*, 2457–2463.

Michaelson, D. M., Horwitz, A. F., & Klein, M. P. (1973) *Biochemistry 12*, 2637–2645.

Nelsestuen, G. L. (1976) *J. Biol. Chem. 251*, 5648–5656.

Nelsestuen, G. L. (1978) *Fed. Proc., Fed. Am. Soc. Exp. Biol. 37*, 2621–2625.
Nelsestuen, G. L., & Broderius, M. (1977) *Biochemistry 16*, 4172–4177.
Nelsestuen, G. L., & Lim, T. K. (1977) *Biochemistry 16*, 4164–4171.
Nelsestuen, G. L., Broderius, M., & Martin, G. (1976) *J. Biol. Chem. 251*, 6886–6895.
Nelsestuen, G. L., Kisiel, W., & DiScipio, R. G. (1978) *Biochemistry 17*, 2134–2138.
Nelsestuen, G. L., Resnick, R. M., Wei, G. J., Pletcher, C. H., & Bloomfield, V. A. (1981) *Biochemistry 20*, 351–358.
Nesheim, M. E., Taswell, J. B., & Mann, K. G. (1979) *J. Biol. Chem. 254*, 10952–10962.
Pletcher, C. H., Resnick, R. M., Wei, G. J., Bloomfield, V. A., & Nelsestuen, G. L. (1980) *J. Biol. Chem. 255*, 7433–7438.
Resnick, R. M., & Nelsestuen, G. L. (1980) *Biochemistry 19*, 3028–3033.
Rosing, J., Tans, G., Govers-Riemslag, J. W. P., Zwaal, R. F. A., & Hemker, H. C. (1980) *J. Biol. Chem. 255*, 274–283.
Smoluchowski, M. (1915) *Ann. Phys. (Leipzig) 48*, 1103.
Smoluchowski, M. (1917) *Z. Phys. Chem., Abt. A 92*, 129.
Williams, R. J. P. (1979) *Biochem. Soc. Trans. 7*, 481.
Yi, P. N., & MacDonald, R. C. (1973) *Chem. Phys. Lipids 11*, 114.

Physical and Biochemical Characterization of a Purified Arginyl-tRNA Synthetase–Lysyl-tRNA Synthetase Complex from Rat Liver†

Chuan Van Dang, Raymant L. Glinski, Philip C. Gainey, and Richard H. Hilderman*

ABSTRACT: Arginyl- and lysyl-tRNA synthetases copurify throughout a six-step chromatographic procedure resulting in a purification of 605- and 559-fold, respectively. The purified enzymes were estimated to be 98% pure with a stoichiometry of 1:1 from acrylamide gel electrophoresis under denaturing conditions. On the basis of a native molecular weight of 285 000 calculated from $s_{20,w}$, R_s, and $\bar{v}$ and subunit molecular weights of 73 000 and 65 000 obtained by sodium dodecyl sulfate gel electrophoresis, the synthetases appear to exist as a tetramer. The tetrameric structure was also supported by cross-linking studies. These results are consistent with an $\alpha_2\beta_2$ structure, but an $\alpha\beta$ structure has not been ruled out.

In general, aminoacyl-tRNA synthetases from mammalian cells have been isolated as partially purified complexes (Bandyopadhyay & Deutscher, 1971; Vennegoor & Bloemendal, 1972; Som & Hardesty, 1975; Denny, 1977; Dang & Yang, 1979; Saxholm & Pitot, 1979) and as multiple forms (Dang & Yang, 1979; Ussery et al., 1977; Roberts & Olsen, 1976). At the present time it is not known if these complexes exist within the cell, nor is the structural basis for these complexes known. Thus, for these questions to be answered, the complexes must be purified to homogeneity so that physical and biochemical studies can be performed.

Accordingly, we have purified a complex which contains only arginyl- and lysyl-tRNA synthetase. Our results suggest that the synthetases exist as a tetramer with a molecular weight of 285 000. Also kinetic studies have been performed on the synthetases. Studies such as these on small complexes are necessary in order to understand larger complexes and the organization of aminoacyl-tRNA synthetases within the mammalian cell.

Experimental Procedures

Materials. Female Long Evans rats (120–150 g) were purchased from Charles River Breeding Laboratories, Inc. All radioisotopes were purchased from Schwarz/Mann. Dimethyl suberimidate dihydrochloride was purchased from Pierce Chemical Co. All other chemicals and supplies were of analytical grade and were obtained from standard chemical sources.

Aminoacyl-tRNA Synthetase Assays. Assays for both arginyl- and lysyl-tRNA synthetase have been optimized and are as follows. Arginyl-tRNA synthetase assays were performed in a volume of 100 μL containing 25 μmol of Hepes,[1] pH 7.0, 0.5 μmol of ATP, 3.5 μmol of $MgCl_2$, 10 μg of bovine serum albumin, >550 μg of unfractionated beef liver tRNA, and 0.025 μmol of [^{14}C]arginine (8–12 cpm/pmol). The reactions were initiated by the addition of the enzyme; after incubation at 37 °C, they were terminated with 3 mL of cold 10% trichloroacetic acid (Cl_3CCOOH) containing 0.02 M sodium pyrophosphate. After 10 min on ice the precipitate was collected on a Whatman R/A glass-fiber filter, washed 6 times with 3-mL portions of 2.5% Cl_3CCOOH containing 0.2 M sodium pyrophosphate and washed 1 time with 5 mL of ethanol–ether (1:1), dried, and counted in a Beckman liquid scintillation counter. A unit is defined as 1 nmol of arginine incorporated/min at 37 °C.

Lysyl-tRNA synthetase assays were performed in a volume of 100 μL containing 25 μmol of Hepes, pH 8.0, 0.5 μmol of ATP, 0.5 μmol of $MgCl_2$, 10 μg of bovine serum albumin, 650 μg of unfractionated beef liver tRNA, 0.02 μmol of EDTA, 0.5 μmol of KCl, and 0.025 μmol of [^{14}C]lysine (8–12

† From the Department of Biochemistry, Clemson University, Clemson, South Carolina 29631. *Received April 15, 1981; revised manuscript received October 13, 1981.* Supported by a Biomedical Research Support Grant Program, Division of Research Resources, National Institutes of Health.

[1] Abbreviations: Hepes, 4-(2-hydroxyethyl)-1-piperazineethanesulfonic acid; ATP, adenosine 5′-triphosphate; EDTA, ethylenediaminetetraacetic acid; DEAE, diethylaminoethyl; Tris, tris(hydroxymethyl)aminomethane; $NaDodSO_4$, sodium dodecyl sulfate.

0006-2960/82/0421-1959$01.25/0 © 1982 American Chemical Society